Comparison of Large-Scale Fading Models with RSRP Measurements

Agnes Fastenbauer*†, Lukas Eller*†, Philipp Svoboda*†, and Markus Rupp†
*Christian Doppler Laboratory for Digital Twin Assisted AI for Sustainable Radio Access Networks
†Institute of Telecommunications, TU Wien, Austria
agnes.fastenbauer@tuwien.ac.at

***Abstract*—Ray tracing methods are gaining popularity for modeling the propagation conditions of wireless links. This adds them to a series of propagation models for wireless channels, making the choice of the appropriate model difficult. This paper evaluates the reliability of several large-scale fading models by comparison with reference signal received power (RSRP) measurements obtained through a drive test in a low-rise urban environment in the 1.855 GHz band. The models integrate different levels of information regarding the link environment. The results show that all models underestimate the propagation loss and that an increase in available information about the environment does not always enhance the accuracy of a model. For system-level simulation, a statistical approach shows the best results, especially in absence of reliable environmental data.**

***Index Terms*—cellular network, fading, large-scale fading, macroscopic fading, measurements, mobile communications, path loss model, propagation loss, ray tracing, reference signal received power, RSRP, shadow fading, shadowing, simulations, system-level, wireless network**

I. Introduction

Knowing the propagation conditions in a wireless channel is necessary for designing efficient transmission schemes and reliable networks. A broad range of propagation models is available to describe the propagation channel in different scenarios. This makes it difficult for authors to find a trusted baseline for investigation and leaves them repeating the same work for different models [1].

In recent years, ray tracing methods have gained popularity [2], because they allow the investigation of high frequency bands without the cost of associated measurements. For millimeter wave (mm-wave) channels, ray tracing has been found to be sufficiently reliable provided the modeling information is accurate [3]; the antenna pattern information plays a significant role in these highly directive channels. Despite the strong reliance on often unavailable accurate data, ray tracing replaces measurements for developing new models [4]. Ray tracing also comes with a significant computational cost.

When computational efficiency is of concern, the 3rd Generation Partnership Project (3GPP) [5], European Cooperation in Science and Technology (COST) [6] and International Telecommunication Union (ITU) [7] offer a range of conventional propagation models defined for different environments, such as urban, rural, or indoor. These models are a trusted baseline for investigations [8].

This paper focuses on large-scale fading models and investigates their accuracy for a vehicular channel in an urban environment at 1.855 GHz. RSRP measurements from a drive test in Vienna, Austria, serve as ground truth for the evaluation of the propagation models (Section II). The investigation considers a statistical model, a 3GPP path loss model, two proposed variations of this 3GPP model, and the MATLAB ray tracer (Section III).

The amount of information about the transmission environment increases with each model. Starting with information about the transmitter and receiver position and adding information about the type of environment, the line of sight (LOS) or non line of sight (NLOS) state of the link, and finally, the buildings of the city. One aim of this comparison is to evaluate how well the models perform with readily available knowledge that is not based on additional measurement campaigns. Hence the model parameters are not tuned to fit the measurement results, but general values are considered. The focus on system-level simulations allows us to trade the accuracy of the modeling of individual links for the accuracy of the network behavior.

It is expected that feeding more information about the link environment to the model leads to more accurate results at the cost of more complexity. This expectation is not met in this investigation. The measurements of one base station sector are qualitatively compared to the propagation loss calculated using the models (Section IV-A), and the empirical cumulative distribution functions (ECDFs) of the estimated and measured reference signal received power (RSRP) values are compared in Section IV-B to evaluate the model accuracy on system level. The results show that statistical approaches can model the network behavior well and that information about the link environment is only enhancing the model performance if the information is accurate and used effectively.

II. Measurement Campaign

The measurement results were obtained through a drive test, that collects the reported RSRP of all base stations received at the user at a frequency of 1.855 GHz with 20 MHz bandwidth. The dataset contains RSRP values from $143,581$ user positions collected from the three sectors of 33 base stations, corresponding to data from 99 cells. This dataset is extensive and includes measurements from the serving cell and other cells. The drive test was performed in Vienna, Austria in a low-rise urban environment. The measurement campaign is described in [9], [10]. An example of the measurement result

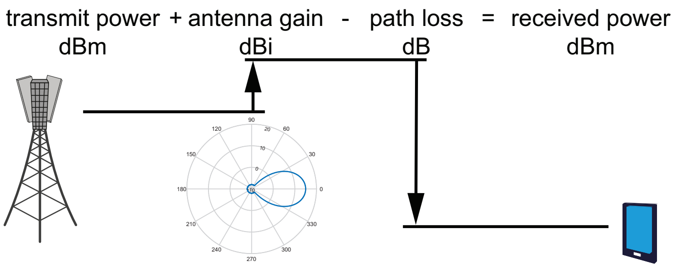

Fig. 1. Link budget for RSRP calculation.

of one sector of a single base station is shown in the upper left map in Fig. 2. It shows the base station and user locations with their associated RSRP value, as well as the antenna orientation and the city geometry.

The RSRP values are standardized in 3GPP TS 36.214 [11]. They are the average power received in the cell-specific reference symbols over the measurement bandwidth. The RSRP values are reported in a range from -44 dBm to -140 dBm. Lower values are not reported and higher values are reported as the maximum RSRP. In the following, it will be assumed that small-scale fading is not visible in the RSRP values due to the averaging over reference symbols.

III. Propagation Models

The link budget used in this investigation is shown in Fig. 1. A link is modeled as a transmitter - with an antenna pattern and a transmit power P_{tx} - linked to a receiver, where the link is affected by large-scale fading L. The user is assumed to be equipped with an omnidirectional antenna with 0 dBi gain in all directions. The RSRP corresponds to the received power at the user P_{rx} and can be expressed as

$$P_{\mathrm{rx}}\big|_{\mathrm{dBm}} = P_{\mathrm{tx}}\big|_{\mathrm{dBm}} + G\big|_{\mathrm{dBi}} - L\big|_{\mathrm{dB}}. \tag{1}$$

The transmit power at the base station P_{tx} and antenna orientation are obtained from the measurement campaign. The antenna gain G is modeled according to [12]. The propagation loss or path loss L is modeled using the models described below.

A. Shadow Fading Model

The shadowing model uses little information about the link and its surroundings. Only the base station and user positions from the measurement campaign are used. The propagation loss is modeled as a combination of free space path loss L_{FSPL} with path loss exponent $\alpha = 2$ and log-normal shadow fading S with mean μ and standard deviation σ. The shadow fading is correlated as explained in [13]. Table I summarizes the model parameters.

The total propagation loss L_{shadow}, used as L in Eq. (1), is calculated as

$$L_{\mathrm{shadow}}\big|_{\mathrm{dB}} = L_{\mathrm{FSPL}}(\alpha)\big|_{\mathrm{dB}} + S(\mu,\sigma)\big|_{\mathrm{dB}}. \tag{2}$$

This model offers a trusted approach to describe the distribution of the propagation loss values. The downside of this model is that it does not capture specific network geometries.

TABLE I
Shadowing model parameters

Free Space Path Loss and Log-Normal Shadowing	
path loss exponent α	2
mean shadowing μ	17 dB
shadowing standard deviation σ	9 dB
decorrelation distance	$40\ln(2)$ m
map correlation	0.5

B. 3GPP Path Loss Model

3GPP offers path loss models for many different scenarios. The urban microcell street canyon model from [5, section 7.4] has been found to be best suited to describe the measurement dataset. The measured base station heights exceed the 10 m base station height prescribed in the model, and the measured transmit powers do not correspond to the transmit power of a microcell. Other 3GPP models were considered for this investigation but showed a worse match with the measurement results.

The 3GPP model defines a LOS path loss and a NLOS path loss, as well as a LOS probability. The LOS probability is used to determine whether a user has a LOS or NLOS connection to the base station. This random LOS decision selects the expression used to determine the propagation loss L_{3GPP}.

The 3GPP urban micro street canyon model is intended to be used in combination with log-normal shadowing with a standard deviation of $\sigma = 4$ dB. The shadowing is not considered in this investigation.

C. 3GPP Path Loss Model with Deterministic LOS Decision

The 3GPP model described above is now extended with a deterministic LOS decision. The LOS decision is based on geometry data extracted from the open street maps database [14]. The interface of the Vienna 5G System-Level Simulator [15] is used to extract the geometry information from the database. The propagation loss L_{detLOS} is then evaluated with the path loss expressions of the 3GPP urban micro street canyon model.

The LOS decision is based on whether the direct line between base station and user passes through a wall of a building from the geometry data. If any wall obstructs the direct line between the base station and the user, the link is considered to be NLOS. Otherwise, the link is considered to be LOS.

The open streets maps database is an open-source database where the open-source community adds information about buildings. Thus, the quality of the data entries can vary. For example, the height of buildings is only sometimes available. To fill the gap, the building heights are randomly set within the range specified by the zoning plan of the region in which the measurements took place. The maximum building height is 21 m, and the minimum is 9 m. All buildings are created with flat roofs, which does not accurately represent the measurement scenario.

D. 3GPP Path Loss Model with Wall Loss

The evaluation showed that the previous model failed to match the measurements. As a remedy, a geometrical fading model is proposed here that extends the 3GPP path loss model with deterministic LOS decision from the previous section with a wall loss L_{wall}. The model is a compromise between the complexity of ray tracing tools and the lack of knowledge about the environment of conventional models.

The path loss L_{geometry} for this model is determined as

$$L_{\text{geometry}}\big|_{\text{dB}} = L_{\text{detLOS}}\big|_{\text{dB}} + L_{\text{wall}}\big|_{\text{dB}}, \tag{3}$$

where the wall loss is defined as

$$L_{\text{wall}}\big|_{\text{dB}} = \max\left(9\ \text{dB}, \sum_{\text{wall}} 3.5\ \text{dB}\right). \tag{4}$$

The sum in Eq. (4) is over all walls obstructing the direct line between base station and user.

E. MATLAB Ray Tracer

The ray tracer offered by MATLAB version R2023b is used. The environment, including the building heights, is imported from the open street map database by the ray tracing tool. A maximum of 5 reflections are considered since evaluation has shown that further increasing the number of reflections does not impact the results. The maximum number of diffraction is limited to one by the available hardware capabilities; for higher numbers of diffraction, results could not be generated.

To limit complexity, the buildings are generated in the same area as user measurements are available for each cell. This leads to users at the border of the cell not receiving any reflections from the outside of the cell, which can limit result accuracy. The flat roof shape of the buildings increases the inaccuracy of the modeling of diffraction.

IV. Results

The different models are analyzed qualitatively in Section IV-A, by comparing RSRP maps of one representative cell. A statistical evaluation is made in Section IV-B by comparing the ECDFs of the RSRP values generated by each model.

A. RSRP Maps

The results are depicted in Fig. 2. The upper left corner shows the RSRP measurement results of all measured user positions in a selected base station sector. The other maps show the RSRP values produced by the different models. The black lines in the maps are the outlines of the buildings; the colored dots represent the measured user positions and their RSRP value. The diamond shape represents the base station, with the gray arrow pointing in the direction of the antenna orientation. A region of size 800 m $\times$ 800 m is shown.

The measurement results show a rather small range of RSRP values with a strong correlation between neighboring measurement positions. Besides the shadowing model, all models underestimate the propagation loss, showing brighter colors than the measurement results. The lower measurement results may, in part, be due to losses in the measurement equipment.

The wave-guiding properties of the streets can only be observed in the models that consider a geometry-based LOS decision. Looking at the third intersection to the right of the base station in the street of the base station, a color change can be observed from the horizontal street to the vertical street. This change is slightly visible in the measurement results and more defined in the maps of the deterministic LOS model, the wall loss model, and the ray tracer. This shows that shadowing effects induced by buildings can be modeled when using geometry information.

The correlation between the distance to the base station and the propagation loss is present in all models. The colors fade to lower RSRP values with increasing distance to the base station in all maps. This behavior stems from the distance-dependent path loss that is present in all models. The influence of the orientation of the antenna can also be observed in all models with slightly brighter colors along the axis of the antenna orientation.

a) Shadowing Model: The colors in the shadowing map in the upper right corner of Fig. 2 match the measurement results best, indicating a good match of the general RSRP range. The spatial distribution of the RSRP values cannot be related to the geometry of the city due to the lack of knowledge about the environment. This shows that the shadowing model is not appropriate for representing specific network geometries, but can be useful to model the overall network behavior.

b) 3GPP Model and Extensions: In the 3GPP model with random LOS decisions, the RSRP values can change strongly from one user position to a neighboring position. This is expected, as the 3GPP model randomly switches between its LOS and NLOS versions. The brighter dots in the 3GPP map become more sparse when moving away from the base station since the LOS probability decreases over distance.

Like the shadowing model, the 3GPP model is unaware of the geometry of the city and cannot reproduce patterns induced by known blockages. However, the simple extension with geometric LOS decision strongly improves the correlation between the measured and the estimated RSRP values.

The addition of a geometry-dependent wall loss remedies the overestimation of the RSRP values of users further away from the base station. In the vicinity of the base station, the estimated RSRP corresponds to the LOS path loss from the 3GPP model.

c) MATLAB Ray Tracer: The results of the MATLAB ray tracing show a lot of variation in the RSRP values from one user position to neighboring user positions. The ray tracer strongly underestimates the propagation loss, but the trends of street tunneling effects correspond to those observed in the measurements.

The same evaluation was also performed with older MATLAB versions, in which diffraction was not yet available. In these investigations, about 15% of user positions could not be traced and produced no results, underlining the strong

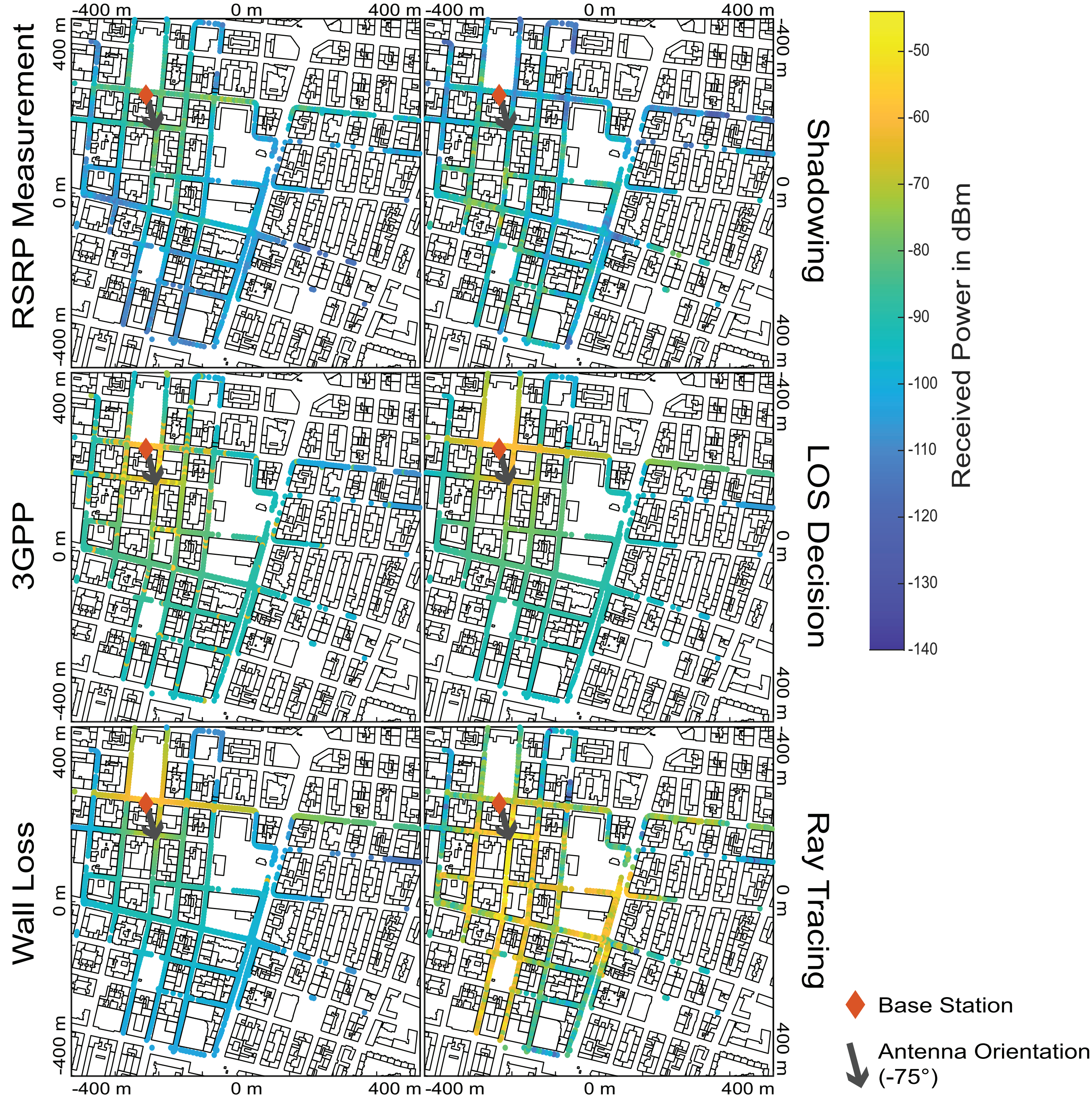

Fig. 2. RSRP maps of a selected base station sector.

influence of diffraction effects in urban environments at sub-6 GHz frequencies.

The discrepancies between the measurements and the ray tracing results could be explained by the inaccurate modeling of the house roof shape, the lack of elevation information in the antenna pattern, or the lack of cars in this vehicular scenario. However, first investigations with the CloudRT ray tracing tool [16], [17] led to more accurate results insinuating that the shortcomings lie in the tool and not the method.

The computational complexity of the ray tracing tool strongly exceeds that of the other models. The simulation duration for a sector was in the order of a few hours for the ray tracer and the order of a minute for the other models. The computational complexity can become prohibitively expensive in system-level simulations considering both desired and interfering links.

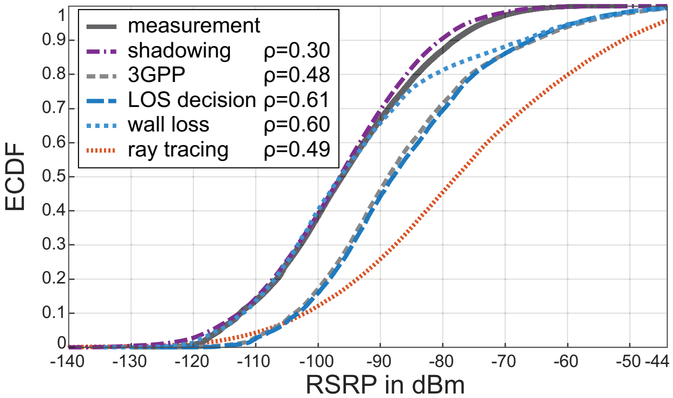

Fig. 3. RSRP ECDFs and correlation coefficient for all models.

B. Statistical Evaluation

This investigation focuses on finding a suitable model for system-level simulation. The system performance is generally described statistically, so this section analyzes the ECDFs of the RSRP values, the errors, and the correlation coefficients between the measurement and the estimated RSRPs. The results are shown in Table II and in Fig. 3.

TABLE II
MODEL ERROR IN dB

	Shadow	**3GPP**	**LOS Dec.**	**Geometry**	**Ray Trace**
$\bar{e}$	1.07	-8.91	-2.14	-9.36	-18.15
MAE	11.8	11.1	9.5	10.8	13.6
RMSE	14.9	14.0	12.0	13.6	17.0

a) Modeling Error: As we have seen in Section IV-A, all models underestimate the propagation loss, except for the shadowing model. The mean error $\bar{e}$, listed in the first line of Table II, is a measure of this systematic error. The table shows that the shadowing and the 3GPP model with deterministic LOS decision have a small error on average, while the other models cannot accurately represent the range of the propagation loss.

The mean error does not adequately represent the error on each measurement position, so we additionally consider the mean absolute error (MAE) and the root mean square error (RMSE) in Table II. For the calculation of the MAE and RMSE, the results are adjusted for the mean error allowing the results to be comparable, despite a possible systematic error due to the measurement equipment. In terms of MAE and RSRP, all models perform poorly; the 3GPP model with deterministic LOS decision performs best with an MAE of 9.5 dB and an RMSE of 12 dB. A deep learning approach on the same dataset was able to achieve an RMSE of about 7 dB [10], showing that the gap between the models and the measurements can be partially closed. The deep learning approach, however, requires measurement data to train the model, which is not required by the models considered here.

Adjusted for the mean error, the model errors lie between -40 dB and 40 dB, an unacceptably large range for the modeling error. Small-scale fading effects neglected in the modeling can partially explain the deviation from the RSRP measurements. However, the observed error is too large to be fully justified by this mechanism. The influence of the small-scale fading on the modeling error is left open to investigation.

b) Correlation Coefficient: The ECDFs in Fig. 3 show a good match between the distribution of the measured values and the estimated RSRP values of the shadowing model. The correlation coefficient of the shadowing model, listed in the legend in Fig. 3, is small and can be seen as a baseline for the correlation to the measurement induced by the distance dependence of the path loss. The correlation coefficient improves slightly for the 3GPP model and the ray tracer to about $\rho = 0.5$. The use of a geometry-based LOS decision doubles the correlation coefficient compared to the shadowing model in the extended 3GPP models with deterministic LOS decision. This shows the significance of LOS state for the propagation conditions.

c) 3GPP Models: The 3GPP model shows a good match of the shape of the ECDF, both with random and deterministic LOS decision. In combination with the increased correlation coefficient, this shows that these models are useful to match real deployments more closely than a purely statistical approach. However, the path loss seems to be strongly overestimated. Additional analysis shows that positions close to the base station show too high RSRP values with errors of about 10 dB, while this error is reduced at positions further away from the base station. This indicates that the 3GPP model has weaknesses in the close vicinity of base stations.

With the wall loss model, a good match can be achieved in the low RSRP regime, showing that the model works well where it is applied. The shape of the wall loss ECDF flattens for RSRP values higher than -80 dBm. This flattening cannot be observed in the measurement results. This discrepancy might stem from the misuse of a micro base station model for a macro base station deployment.

d) MATLAB Ray Tracer: The RSRP values estimated with the MATLAB ray tracer show a different overall behavior than the measurements. Some of the discrepancies can be explained by inaccuracies in the modeling data, which does not consider the shape of the roofs, changes that might have occurred over time, the exact building materials, or the true antenna pattern. The absence of cars in this vehicular scenario might also play a significant role, as shown by [18] for a frequency of 5.9 GHz.

However, an analysis performed with the CloudRT ray tracing tool [16], [17] and more detailed building information, showed a better match with a correlation coefficient of $\rho = 0.7$ and a MAE of 7.3 dB after adjustment for the mean error. This shows that the MATLAB ray tracer can produce large errors and should not be trusted blindly.

The accuracy of ray tracing strongly depends on the availability and accuracy of environmental data. Some environmental data is not static, such as moving cars, and cannot be accurately modeled without constant surveillance of the environment or a statistical model. When relying on statistical descriptions of the propagation channel is necessary, a simple model is already available in the shadowing model. This confirms the findings in [19], which show that semi-empirical models achieve a better fit than ray tracing at a frequency of 2.4 GHz. It should also be noted that the common approach [20], [21] of training machine learning models with data generated by ray tracing tools might not result in useful models.

In terms of computational complexity, the shadowing model and the 3GPP model are the most efficient. The deterministic LOS decision used in the extensions of the 3GPP increases the simulation time by about 20%. The ray tracing increases the simulation duration by a hundredfold, or about 10000%.

V. Conclusion

Comparison of estimated RSRP values with measurements has shown that all considered large-scale fading models result in an RMSE above $10\ \mathrm{dB}$. Such large errors are common in large-scale fading modeling, even when considering ray tracing methods with detailed environment models. In the context of system-level simulation, statistical models are shown to be the most appropriate choice, as they offer low computational complexity and a good fit to the overall network behavior. When specific geometries are of interest, the determination of the LOS property of links according to the specified geometry is an efficient way to increase the accuracy of the model, reducing the RMSE by almost $3\ \mathrm{dB}$ compared to the shadowing model.

The comparison has also shown that ray tracing models can be affected by large errors ($17\mathrm{dB}$ RMSE) and should not be used as the basis for the development of new models as is commonly done in literature. Ray tracing requires accurate and detailed modeling of the environment, but this information is often unavailable, rendering ray tracing results inaccurate.

In conclusion, simpler models should be preferred to the ray tracing approach, especially in the absence of detailed and accurate environmental information or when computational efficiency is of concern.

Acknowledgment

This work has been funded by the Christian Doppler Laboratory for Digital Twin assisted AI for sustainable Radio Access Networks. The financial support by the Austrian Federal Ministry for Digital and Economic Affairs, the National Foundation for Research, Technology and Development and the Christian Doppler Research Association is gratefully acknowledged.

References

[1] M. U. Sheikh, R. Jantti, and J. Hamalainen, "Impact of interference suppression under ray tracing and 3GPP street canyon model," in *2020 IEEE 91st Vehicular Technology Conference (VTC2020-Spring)*. IEEE, May 2020.

[2] N. Moraitis and K. S. Nikita, "Ray-tracing propagation modeling in urban environment at 140 GHz for 6G wireless networks," *IEEE Access*, vol. 11, 2023.

[3] A. Schott, A. Ichkov, P. Mähönen, and L. Simić, "Measurement validation of ray-tracing propagation modeling for mm-wave networking studies: How detailed is detailed enough?" in *2023 17th European Conference on Antennas and Propagation (EuCAP)*, 2023, pp. 1–5.

[4] O. A. Topal, M. Ozger, D. Schupke, E. Björnson, and C. Cavdar, "mmWave communications for indoor dense spaces: Ray-tracing based channel characterization and performance comparison," in *ICC 2022 - IEEE International Conference on Communications*, 2022, pp. 516–521.

[5] 3rd Generation Partnership Project (3GPP), "Technical specification group radio access network; study on channel model for frequencies from 0.5 to 100GHz," TR 38.901, Dec. 2017.

[6] E. Commission, D.-G. for the Information Society, and Media, *COST Action 231 – Digital mobile radio towards future generation systems: Final Report*. Publications Office, 1999.

[7] ITU, "Guidelines for evaluation of radio transmission technologies for IMT-2000," Rec. M.1225, 1997.

[8] E. Aksoy, H. Khan, Y. Chen, L. Raschkowski, L. Thiele, and S. Stanczak, "Accurate vegetation models with low computational complexity for ray tracing," in *2023 International Microwave and Antenna Symposium (IMAS)*. IEEE, Feb. 2023.

[9] L. Eller, P. Svoboda, and M. Rupp, "Propagation-aware Gaussian process regression for signal-strength interpolation along street canyons," in *2021 IEEE 93rd Vehicular Technology Conference (VTC2021-Spring)*. IEEE, Apr. 2021.

[10] ——, "A deep learning network planner: Propagation modeling using real-world measurements and a 3D city model," *IEEE Access*, vol. 10, pp. 122 182–122 196, 2022.

[11] 3rd Generation Partnership Project (3GPP), "Evolved universal terrestrial radio access (E-UTRA); physical layer; measurements," TS 36.214, Sep. 2022.

[12] ——, "Evolved universal terrestrial radio access (E-UTRA); radio frequency (RF) system scenarios," TR 36.942, Mar. 2017.

[13] T. Dittrich, M. Rupp, and M. Taranetz, "An Efficient Method for Avoiding Shadow Fading Maps in System Level Simulations," in *WSA 2017; 21st International ITG Workshop on Smart Antennas*, Mar. 2017, pp. 1–8.

[14] "OpenStreetMap," https://www.openstreetmap.org/, accessed: 2024-01-07.

[15] M. K. Müller, F. Ademaj, T. Dittrich, A. Fastenbauer, B. R. Elbal, A. Nabavi, L. Nagel, S. Schwarz, and M. Rupp, "Flexible multi-node simulation of cellular mobile communications: the Vienna 5G System Level Simulator," *EURASIP Journal on Wireless Communications and Networking*, vol. 2018, no. 1, p. 17, Sep. 2018.

[16] D. He, B. Ai, K. Guan, L. Wang, Z. Zhong, and T. Kürner, "The design and applications of high-performance ray-tracing simulation platform for 5G and beyond wireless communications: A tutorial," *IEEE Communications Surveys & Tutorials*, vol. 21, no. 1, pp. 10–27, 2019.

[17] D. He, K. Guan, D. Yan, H. Yi, Z. Zhang, X. Wang, Z. Zhong, and N. Zorba, "Physics and AI-based digital twin of multi-spectrum propagation characteristics for communication and sensing in 6G and beyond," *IEEE Journal on Selected Areas in Communications*, vol. 41, no. 11, pp. 3461–3473, Nov. 2023.

[18] M. Ansari, L. Thielecke, and T. Kürner, "Evaluating ray-tracing versus channel-sounder measurements in vehicular communications," in *2023 IEEE 98th Vehicular Technology Conference (VTC2023-Fall)*. IEEE, Oct. 2023.

[19] A. P. Yuste, J. Llumiquinga Pachacama, and J. S. García, "Characterization of the 2.4 GHz-band using a semiempirical model and a ray tracing model," in *2023 IEEE Conference on Antenna Measurements and Applications (CAMA)*. IEEE, Nov. 2023.

[20] W. Xing, T. Su, Y. Yang, and W. Zhao, "Accuracy analysis of urban propagation prediction using ray tracing and machine learning," in *2023 International Conference on Microwave and Millimeter Wave Technology (ICMMT)*. IEEE, May 2023.

[21] Y. Zheng, S. Li, T. Su, K. Chi, Y. Yang, and W. Xing, "An efficient wave propagation prediction model generated by CycleGAN with ray tracing data," in *2023 IEEE 6th International Conference on Pattern Recognition and Artificial Intelligence (PRAI)*. IEEE, Aug. 2023.